JOURNAL OF QUATERNARY SCIENCE (2006) **21**(2) 115–130

Published online 27 October 2005 in Wiley InterScience (www.interscience.wiley.com). DOI: 10.1002/jqs.955

Glacier response in the European Alps to Heinrich Event 1 cooling: the Gschnitz stadial

SUSAN IVY-OCHS,[1]* HANNS KERSCHNER,[2] PETER W. KUBIK[3] and CHRISTIAN SCHLÜCHTER[4]
[1] Teilchenphysik, ETH-Hönggerberg, CH-8093 Zurich, Switzerland, and Geographisches Institut, Universität Zurich-Irchel, CH-8057 Zurich, Switzerland
[2] Institut für Geographie, Universität Innsbruck, A-6020 Innsbruck, Austria
[3] Paul Scherrer Institut c/o Teilchenphysik, ETH-Hönggerberg, CH-8093 Zurich, Switzerland
[4] Geologisches Institut, Universität Bern, CH-3012 Bern, Switzerland

Ivy-Ochs, S., Kerschner H., Kubik, P. W. and Schlüchter, C. 2005. Glacier response in the European Alps to Heinrich Event 1 cooling: the Gschnitz stadial. *J. Quaternary Sci.*, **Vol. 21** pp. 115–130. ISSN 0267-8179.

Received 17 January 2005; Revised 31 May 2005; Accepted 6 June 2005

ABSTRACT: The Gschnitz stadial was a period of regionally extensive glacier advance in the European Alps that lies temporally between the breakdown of the Last Glacial Maximum piedmont lobes and the beginning of the Bølling warm interval. Moraines of the Gschnitz stadial are found in medium to small catchments, are steep-walled and blocky, and reflect a snowline lowering of 650–700 m in comparison to the Little Ice Age reference snowline. ^{10}Be surface exposure dating of boulders from the moraine at the type locality at Trins (Gschnitz valley, Tyrol, Austria) shows that it stabilised no later than 15 400 ± 1400 yr ago. The overall morphological situation and the long reaction time of the glacier suggest that the climatic downturn lasted about 500 ± 300 yr, indicating that the Gschnitz cold period began approximately 15 900 ± 1400 yr ago, if not somewhat earlier. This is consistent with published radiocarbon dates that imply that the stadial occurred sometime between 15 400 ^{14}C yr BP (18 020–19 100 cal. yr) and 13 250 ^{14}C yr BP (15 360–16 015 cal. yr). A palaeoclimatic interpretation of the Gschnitz glacier based on a simple glacier flow model and statistical glacier-climate models shows that precipitation was about one-third of modern-day precipitation and summer temperatures were about 10 K lower than today. In comparison, during the Younger Dryas, precipitation in this area was only about 10% less and T_s (summer temperature) was only 3.5–4 K lower than modern values. Based on the age of the moraine and the cold and dry climate at that time, we suggest that the Gschnitz stadial was the response of Alpine glaciers to cooling of the North Atlantic Ocean associated with Heinrich Event 1. Copyright © 2005 John Wiley & Sons, Ltd.

KEYWORDS: Alpine Lateglacial moraines; cosmogenic ^{10}Be; surface exposure dating; Oldest Dryas.

Introduction

Following the peak of the Last Glacial Maximum (LGM) the piedmont lobes that covered the Alpine foreland disintegrated rapidly (e.g. Schlüchter, 2004; van Husen, 2004) into large valley glaciers, that in the higher regions comprised dendritic glacier systems. On the foreland, lakes and bogs formed. This transition marks the beginning of the Oldest Dryas (Greenland Stadials 2b and 2a; Björck *et al.*, 1998; Walker *et al.*, 1999), which lasted until the start of the Bølling 14 700 yr ago (Greenland Interstadial 1). As defined by Penck and Brückner (1901/1909) the 'Alpine Lateglacial' (starting with the Oldest Dryas) began as soon as the foreland piedmont glaciers had melted back into the mountains after the peak of the LGM. Detailed sedimentological and palynological investigations show that before the beginning of the Bølling a number of distinct cold periods can be identified (e.g. Welten, 1982; Amman *et al.*, 1994; Burga and Perret, 1998). Similarly, moraine sets in the alpine valleys indicate repeated expansions of glaciers during the Oldest Dryas. Linkage of climate downturns identified in the pollen record with glacier fluctuations as demarcated by the moraines has been nearly impossible because of dating difficulties (cf. Preusser, 2004).

The most marked of the glacier readvances before the beginning of Bølling is recorded by the family of moraines known as 'Gschnitz'. It is the aim of this paper to establish when the Gschnitz cold event occurred and what the climate was like at that time. To date directly the end of the Gschnitz stadial we chose to exposure date boulders from the type locality at Trins, Austria, using *in situ* produced ^{10}Be (Lal, 1991; Gosse and Phillips, 2001). To get a picture of what the climate was like during the Gschnitz stadial we used glaciological modelling (cf. Kerschner *et al.*, 1999) of the former Gschnitz glacier as defined by the Trins moraine. From this we derived

* Correspondence to: Susan Ivy-Ochs, Teilchenphysik, ETH-Hönggerberg, CH-8093 Zurich, Switzerland and Geographisches Institut, Universität Zurich-Irchel, CH-8057 Zurich, Switzerland. E-mail: ivy@phys.ethz.ch

quantitative palaeoclimatic conditions (summer temperature and precipitation) for a period of time, the early Lateglacial, about which very little is presently known. We hope to shed light on the temporal relationship between the regionally extensive glacier advance that led to build-up of Gschnitz stadial moraines in the European Alps and distinctive climate events as seen in North Atlantic Ocean sediment cores (e.g. Bond *et al.*, 1992; Hemming, 2004) and Greenland ice core records (e.g. Johnsen *et al.*, 2001). This will provide crucial information for the understanding of trigger and transfer mechanisms in the Earth's climate system (Broecker, 2003). The Alps lie in an especially sensitive downwind position with respect to the North Atlantic Ocean. Major changes in ocean circulation, sea surface temperatures and sea-ice coverage should be reflected in almost instantaneous changes in glacier volumes in the European Alps (e.g. Florineth and Schlüchter, 2000).

The Alpine Lateglacial stadials

No later than 21 000–19 000 yr BP (Ivy-Ochs *et al.*, 2004), the LGM system of ice domes (Florineth and Schlüchter, 1998, 2000; Kelly *et al.*, 2004), outlet glaciers and piedmont glaciers that extended onto the foreland of the European Alps had begun to break down (Schlüchter, 1988, 2004; van Husen, 1997, 2000, 2004). Quite soon after the peak of the LGM, large parts of the central Alps were free of ice (e.g. van Husen, 2000) and huge systems of dendritic glaciers existed. With time, these gave way to glaciers filling just the main longitudinal valleys (e.g. Inn and Rhône) and finally to local valley and cirque glaciers (Penck and Brückner, 1901/1909; van Husen, 2000). This general downwasting trend was interrupted by a number of successively smaller glacier readvances known as the 'Lateglacial stadials' (Table 1). Numerous moraine systems in valleys and cirques, which have been mapped over wide areas of the Alps since the second half of the 19th century, document the Alpine Lateglacial stadials. The assignment of moraines to a stadial is based on a number of diagnostic features: (i) relative position of the moraines; (ii) moraine morphology and related periglacial features; (iii) equilibrium line altitude (ELA); and (iv) depression of the ELA (δELA) relative to the Little Ice Age (LIA) ELA (e.g. Penck and Brückner, 1901/1909; Heuberger, 1966; Gross *et al.*, 1977; Maisch, 1981, 1987, 1992). The presently used terminology for the Alpine Lateglacial (Heuberger, 1966; Mayr and Heuberger, 1968; Patzelt, 1972; Maisch, 1982, 1987, 1992; Kerschner, 1986; van Husen, 1997, 2000, 2004) is based on the system originally set up by Penck and Brückner (1901/1909). With the exception of the Egesen stadial, which was verified to be Younger Dryas (Greenland Stadial 1) in age (Ivy-Ochs *et al.*, 1996, 1999), the absolute ages of the Lateglacial stadials are still unclear. Numerous minimum radiocarbon ages suggest that all of them, except the Egesen and Kromer/Kartell, occurred during the Oldest Dryas. The final glacier advances (Kromer/Kartell) may have even actually occurred during the early Holocene.

The Gschnitz stadial

Gschnitz type moraines of tributary valley glaciers are widespread in both the Eastern (Mayr and Heuberger, 1968; Patzelt, 1975; Gross *et al.*, 1977; van Husen, 1977, 1997, 2000, 2004) and Western Alps (Maisch, 1981, 1982, 1987, 1992). They are mainly found in areas where glaciers were several tens to a few hundred square kilometres in size. In the higher areas of the Alps, like the Valais, the Mont Blanc massif and the Bernese Oberland, very large dendritic glacier systems probably still existed. Key sites in the Eastern Alps include the Traun valley, the Pinzgau (upper part of the Salzach river catchment), the Gerlos pass area (van Husen, 2000 and references therein) and the Trins moraine (type locality: Penck and Brückner 1901/1909) discussed here. In the Western Alps, Gschnitz moraines were described by Brückner (Penck and Brückner, 1901/1909), but only in catchments of typical 'Eastern Alpine' extent and morphology (see also Maisch, 1981; Müller *et al.*, 1981; Renner, 1982; Müller, 1984; Schoeneich, 1998). Notable Gschnitz moraines in the Graubünden region are found for example near Davos (Sertig glacier; Maisch, 1981), and Airolo (Bedretto glacier; Renner, 1982). In wide areas of the Alps, particularly in the Western Alps, the extent of the Gschnitz Stadial is not well known. Even after almost a century of mapping, Gschnitz moraines have not been found in the large longitudinal valleys of the Alps (e.g. the Rhône valley, the upper Aare valley and its tributaries, or the Inn valley). In general, the overview of Gschnitz glacier extents given by Brückner (Penck and Brückner, 1901/1909) is still largely valid.

Based on information obtained from Gschnitz stadial moraines in the central and Eastern Alps, Gschnitz stadial glaciers exhibited a δELA in the order of 650–700 m relative to the Little Ice Age ELA (Patzelt, 1975; Gross *et al.*, 1977; van Husen, 1977; Maisch, 1981, 1982, 1987; Müller *et al.*, 1981; Renner, 1982; Kerschner and Berktold, 1982; Müller, 1984; Wetter, 1987; Kerschner, 1993). In comparison, the ELA depression associated with the LGM glaciers was in the order of 1200 m (e.g. Maisch, 1987; Haeberli, 1991; van Husen, 1997, 2000). Because LGM glaciers fanned out into piedmont lobes on the foreland, the area and volume differences (see Fig. 1) were much more pronounced.

Gschnitz stadial moraines (at altitudes below 1400 m) frequently are characterised by a rather sharp-crested morphological appearance with only minor signs of periglacial reworking. The moraines are often several tens of metres high and contain abundant coarse and blocky debris. In suitable locations they are connected to well-developed outwash terraces (van Husen, 1977). Basal till overlying glacifluvial gravels (van Husen, 1977) or rockslide deposits (Kerschner and Berktold, 1982) shows that Gschnitz glaciers advanced several kilometres over ice-free terrain.

The moraine at Trins

The moraine near the village of Trins (latitude 47° 4′43′ and longitude 11° 25′2′, 1200 m) in the Gschnitz valley was chosen as the type locality of the Gschnitz stadial by Penck and Brückner (1901/1909). It is situated 30 km to the south of Innsbruck and about 150 km south of the LGM end moraines of the Inn glacier system (Fig. 1). Various authors have studied the glacial geomorphology of the Gschnitz valley (e.g. Pichler, 1859; Kerner von Marilaun, 1890; Paschinger, 1952; Senarclens-Grancy, 1958; Mayr and Heuberger, 1968), defining and redefining the Lateglacial system of glacier advances of the Eastern Alps in general and that of the Gschnitz valley in particular (cf. Mayr and Heuberger, 1968; Kerschner, 1986; Patzelt and Sarnthein, 1995).

The moraine complex at the type locality in Trins consists of an arcuate end-moraine complex with lateral moraines and

Table 1 Summary of characteristics of deposits and regional situation of glaciers for the Lateglacial stadials, European Alps

Stadial	Moraine morphology	Regional situation	ELA depression	Time-stratigraphic position
Kromer/Kartell	Well-defined, blocky, multi-walled moraines, small rock glaciers. Type localities in the Ferwall group (Kartell cirque (10)) and Silvretta group (Kromer valley (7)).	Cirque and valley glaciers, clearly larger than LIA, but smaller than innermost Egesen phase.	−120 to −60 m depending on location (7, 11, 24).	Unclear, perhaps early Holocene (24). Time-stratigraphic equivalence of Kromer and Kartell presently under discussion.
Egesen	Sharp-crested, often blocky, multi-walled moraines (2). Three-phased readvance of valley glaciers and cirque glaciers; development of extensive rock glacier systems during later parts of the stadial (22, 24, 25), well documented in wide areas of the Alps. Type locality in the Stubai valley SW of Innsbruck (2).	Cirque and valley glaciers, few dendritic glaciers (23).	−450 to −180 m for the maximum advance, depending on location (22).	Younger Dryas (e.g. 4, 17, 18).
Bølling–Allerød Interstadial	No field evidence for glacial advances, although various climatic fluctuations (colder phases) should have caused glaciers to advance. Deposits of the advances were prbably overrun during Younger Dryas (20).	Cirque and valley glaciers (?).	Less than Egesen (20).	Bølling–Allerød.
Daun	Well-defined but smoothed moraines, relatively few boulders, solifluction overprint during YD (Egesen) (2); moraines usually missing in more oceanic areas of the Alps (overrun by Egesen?) (23). Smaller than Clavadel/Senders, perhaps 'appendix' of Clavadel/Senders (indirectly 1). Type locality in the Stubai valley SW of Innsbruck (3).	Glaciers slightly larger than local Egesen glaciers.	ca. −400 to −250 m depending on location (7).	Before Bølling (11, 12).
Clavadel/Senders	Well-defined, often sediment-rich moraines (11, 12, 13, 14). Clearly smaller than 'Gschnitz'. Type localities near Davos (Clavadel (11)) and Innsbruck (Senders (14)), probably equivalent to Zwischbergen stadial at Simplon Pass (15, 16).	Cirque and valley glaciers, some dendritic glaciers still intact.	ca. −400 to −500 m depending on location (15, 16).	Before Bølling.
Gschnitz	Steep-walled, somewhat blocky, large single moraines, no solifluction overprint below 1400 m. Widespread readvance of large valley glaciers on a timescale of several centuries (21). Glaciers advanced over ice-free terrain (8, 9, 14). Type locality in the Gschnitz valley South of Innsbruck (3).	Many valley glaciers, some large dendritic glaciers still intact.	ca. −650 to −700 m (7).	Before Bølling (5, 6, 8, 15, 16).

Continues

Table 1 Continued

Stadial	Moraine morphology	Regional situation	ELA depression	Time-stratigraphic position
Phase of early Lateglacial ice decay	General downwasting after collapse of piedmont glaciers in the foreland with some minor oscillations of the glacier margins. Mainly ice marginal deposits, few moraines. Glacial advances also due to ice-mechanical causes (26). Comprises the classical 'Bühl' and 'Steinach' stadials (1, 3, 8, 26).	Downwasting dendritic glaciers (5), increasing number of local glaciers.	Largely undefined, between ± LGM and −800 m.	Before Bølling, older than 15 400 ± 470 ^{14}C yr BP (8).
LGM	Ice domes in the high Alps (27, 28, 29), outlet glaciers and piedmont glaciers on the foreland.	Piedmont lobes.	−1000 to > −1200 m.	Final collapse 21 000–19 000 yr ago (19).

Principal sources: Senarclens-Grancy (**1** 1958), Heuberger (**2** 1966), Mayr and Heuberger (**3** 1968), Patzelt (**4** 1972; **5** 1975; **6** 1995), Gross *et al.* (**7** 1977), van Husen (**8** 1977; **9** 1997), Fraedrich (**10** 1975), Maisch (**11** 1981; **12** 1982; **13** 1987), Kerschner and Berktold (**14** 1982), Müller (**15** 1982; **16** 1984), Kerschner (**17** 1986), Ivy-Ochs *et al.* (**18** 1996; **19** 2004), Ohlendorf (**20** 1998), Kerschner *et al.* (**21** 1999; **22** 2000), Hertl (**23** 2001), Sailer (**24** 2001), Sailer and Kerschner (**25** 1999), Reitner (**26** 2005), Florineth and Schlüchter (**27** 1998; **28** 2000), Kelly *et al.* (**29** 2004). References before early 1950s see Kerschner (1986)

related ice-marginal features (Fig. 2). The latter are almost completely preserved for a distance of more than 3 km upvalley to an altitude of 1410 m (Fig. 3) (Kerner von Marilaun, 1890; Paschinger, 1952). Above the village of Gschnitz, 6–6.5 km from the end moraine, remnants of moraines at altitudes of 1520–1540 m can be traced downvalley to the lateral moraines. The moraine complex was deposited by a glacier that was about 18 km long (Fig. 4) and had a surface area of 51 km^2. On the right-hand side of the river, the end moraine is about 30 m high and 100 m wide. There, the distal front of the moraine falls away at an angle of 30–35°. The surface area of a cross-section through the terminal moraine is in the order of 1500–2000 m^2. At the lowest point, the end moraine is dissected and breached by the present-day river. Apart from that, no signs of strong post-depositional periglacial or fluvial reworking can be seen. A small outwash terrace stretches downvalley for about 500 m. In exposures created during construction over the past 30 years, one can see that the moraine is composed of crystalline till with a considerable amount of Mesozoic carbonates as smaller clasts and in the matrix. Sticking out of the surface of the moraine are subangular to subrounded crystalline boulders (so-called 'Ötztaler Schiefergneis') which are up to several metres in diameter. These are especially abundant along the left-hand side of the end-moraine complex where there are two to three closely spaced parallel ridges and several kettle holes. This surface morphology suggests that the ice on the lower left-hand side of the glacier tongue was thickly covered by crystalline rockfall debris that had been transported on the glacier surface.

Remnants of the Steinach moraine (type locality: Senarclens-Grancy, 1958; Mayr and Heuberger, 1968) lie a few kilometres downstream from Trins near the town of Steinach. Fragmentary remnants of other moraines in the lower Gschnitz valley, which were mentioned by Kerner von Marilaun (1890) and Mayr and Heuberger (1968), have been destroyed during the past few decades.

Timing of the Gschnitz Stadial

^{14}C ages related to the Gschnitz stadial

All published ^{14}C ages that can be linked to the Gschnitz cold event are discussed below (see Fig. 1 for site locations). We describe the site where the material for radiocarbon dating was obtained in relation to the local Gschnitz glacier, because such information was generally not included in the original publications. Our approach is to include minimum radiocarbon ages for moraines which, based on ELA change relative to the LIA ELA as well as geomorphological criteria, we or the listed authors correlate to the Trins-type Gschnitz moraine or to moraines that are younger than Gschnitz but older than Egesen (Younger Dryas). Such correlations are not necessarily unambiguous. Before the onset of the Bølling, most glaciers were rather large, making calculation of ELAs complicated. Thus in some places, possibly Gschnitz stadial moraines may have been confused earlier with moraines of the (stratigraphically younger) Clavadel/Senders stadial (cf. Kerschner, 1986). The radiocarbon ages, including the stated uncertainties, have been converted to calendar ages with IntCal04 (Reimer *et al.* 2004) using the CALIB 5.0.1 software (Stuiver *et al.*, 1998, 2005). The calibrated radiocarbon age ranges are plotted in Fig. 5.

The following radiocarbon ages were obtained from the Krothenweiher peat bog which lies proximal to the Trins moraine crest ('K' in Fig. 3). Bulk sediment samples yielded ages of

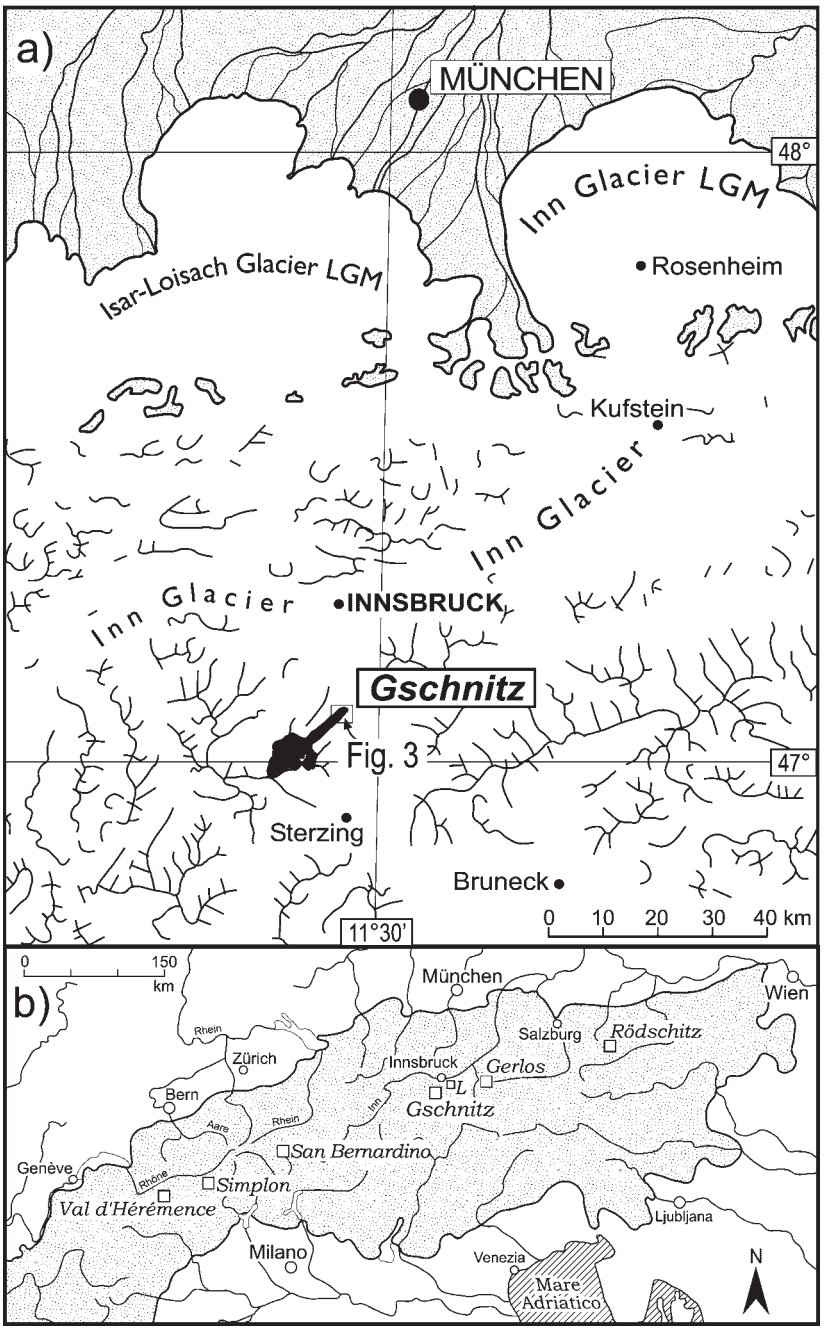

Figure 1 (a) Index map showing the extent of the Gschnitz glacier, LGM glacier extent and crestlines after van Husen (1977). Note the location of Fig. 3, the map of the terminal moraine complex. (b) Location map for sites discussed in the text, L = Lansersee

9635 ± 230 ^{14}C yr BP (10 595–11 250 cal. yr) and 9555 ± 220 ^{14}C yr BP (10 590–11 185 cal. yr) (Bortenschlager, 1984a), while wood fragments gave AMS ^{14}C ages of 9790 ± 110 ^{14}C yr BP (10 880–11 385 cal. yr), 9720 ± 100 ^{14}C yr BP (10 820–11 245 cal. yr) and 9650 ± 100 ^{14}C yr BP (10 795–11 025 cal. yr) (Patzelt and Sarnthein, 1995). These ages were obtained in the gyttja section of the core close to the base of the section. Similarly, pollen analysis showed that organic sedimentation on the proximal side of the moraine did not start before the early Preboreal period (Bortenschlager, 1984a), which began 11 600 yr ago (e.g. Walker *et al.*, 1999).

On the southern side of San Bernardino pass (Graubünden, Switzerland), an age of $13\,010 \pm 200$ ^{14}C yr BP (15 085–16 750 cal. yr) (Zoller and Kleiber, 1971) was obtained from a bog at Suossa di San Bernardino (1700 m). The bog lies in an area previously covered by ice of the Gschnitz stadial glacier tongue or at least in a lateral position very close to the tongue at much higher elevation than the terminus of the San Bernardino Gschnitz glacier (Kerschner, 1977). Higher up at Sass de la Golp (1953 m), on the southern side of San Bernardino pass, pollen analysis indicated that the peat bog existed already in the Oldest Dryas (Burga, 1980). The peat bog is situated in the lower part of the accumulation area of the Gschnitz stadial glacier. Thus the ^{14}C age of $12\,280 \pm 160$ ^{14}C yr BP (13975–14 580 cal. yr) (Burga, 1980) provides a minimum age for the deglaciation of the accumulation area of the glacier. Based on the location of moraines and moraine fragments in this region that are correlative to the Clavadel stadial (Kerschner, 1977), we conclude that this data might also give a minimum age for Clavadel in the San Bernardino region.

Pollen analysis at Hopschensee (Simplon pass, Switzerland, 2017 m; Welten 1982) indicates that bottom sediments

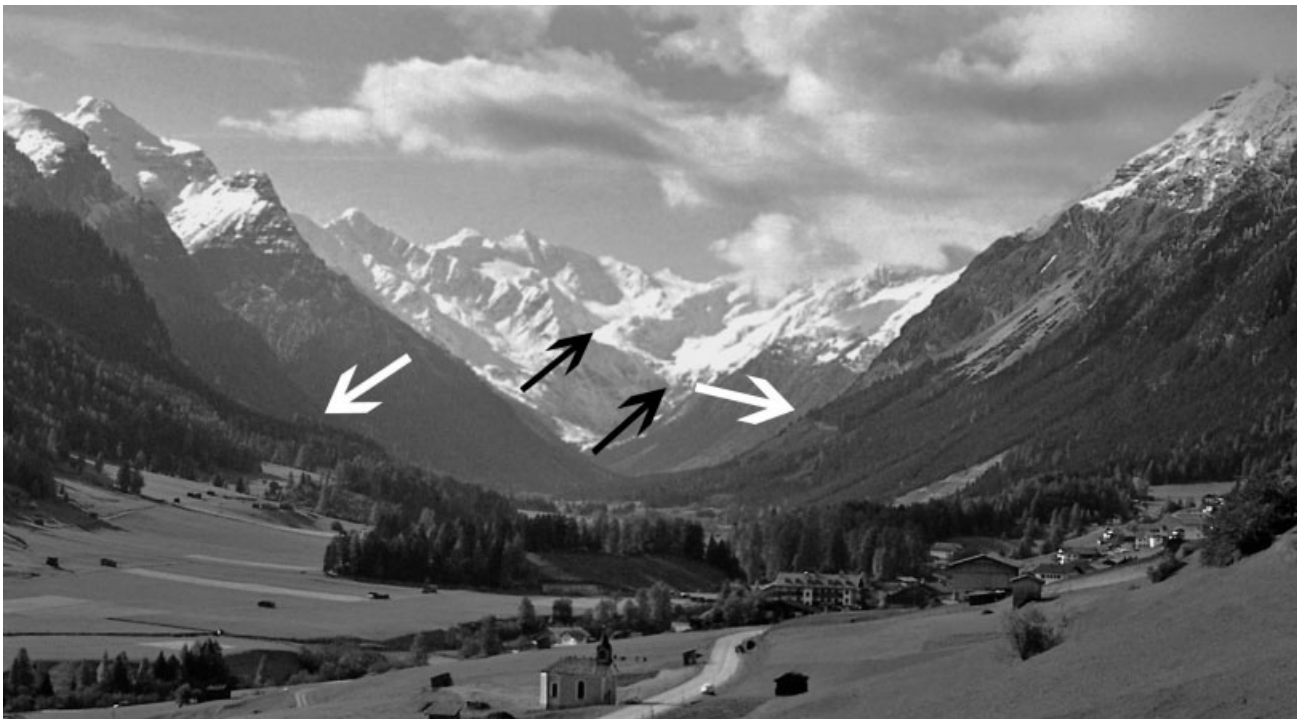

Figure 2 View of the moraine arc of Trins, Gschnitz valley, Tyrol, Austria. The end moraine is represented by the forested ridge crossing the valley in the foreground. Altitude of end moraine crestline above chapel is 1230 m. White arrows mark uppermost position of quasi-continuous lateral moraines. Lower black arrow marks position of Egesen Stadial (Younger Dryas) glacier end, upper black arrow gives approximate position of LIA glacier end of Simmingferner (hidden behind bedrock ridge). Highest peaks in the background are between 2900 m and 3200 m (photo: H. Kerschner)

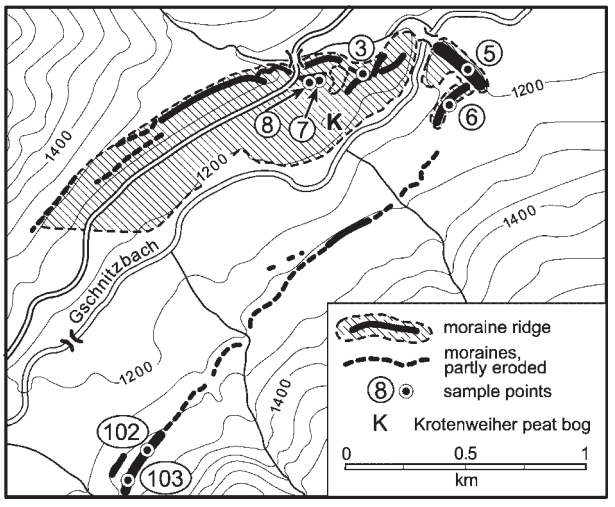

Figure 3 Map of the terminal moraine complex at Trins Austria with locations of boulders sampled

pre-date the start of the Bølling. The oldest radiocarbon age obtained was 12 580 ± 200 ^{14}C yr BP (14 300–15 510 cal. yr) (Welten, 1982). Hopschensee is located within the lower part of the accumulation area of the Gschnitz (Gondo) stadial glacier of the Simplon area (Müller, 1984).

Further to the west in canton Valais a basal date of 12 085 ± 200 ^{14}C yr BP (13 695–14 220 cal. yr) in the Gouillé Rion peat bog at Alp d'Essertse (2342 m) in the Val d'Hérémence (Tinner *et al.*, 1996) provides a minimum-limiting age for moraines which can be attributed to the Clavadel or Daun stadial. The respective glacier, with a snowline only 310 m below that of the Little Ice Age (Tinner *et al.*, 1996), was clearly much smaller than the Gschnitz stadial glacier. According to Brückner (Penck and Brückner, 1901/1909), the terminus of the Gschnitz glacier would have been near the mouth of the valley, at around 850 m.

At Gerlos pass (Salzburg, Austria, 1590 m), ages of 12 290 ± 110 ^{14}C yr BP (14 000–14 450 cal. yr) and 12 155 ± 210 ^{14}C yr BP (13 755–14 400 cal. yr) were obtained (Patzelt, 1975; Bortenschlager, 1984a). The sampling site and its surroundings were subjected to intense periglacial activity during the Gschnitz stadial which prohibited peat bog growth. Therefore, these ages give a minimum age for the Gschnitz (Gerlos) stadial (Patzelt, 1975).

Radiocarbon ages of 13 980 ± 240 ^{14}C yr BP (16 290–17 040 cal. yr), 13 230 ± 190 ^{14}C yr BP (15 360–15 965 cal. yr) and 13 250 ± 210 ^{14}C yr BP (15 360–16 015 cal. yr) were obtained from the peat bog at Lanser See (840 m) near Innsbruck (Patzelt, 1995). The peat bog is situated about 15 km north and 350 m lower in elevation than the Trins Gschnitz moraine. It is likely that the 13 980 ^{14}C yr BP date is too old, because it is incongruent with the age–depth model (see also Patzelt, 1995); therefore we disregard it below as a minimum age. However, it should be mentioned that the sediment dated to 13 980 ^{14}C yr BP does underlie sediment that contains pollen which indicate a climatic downturn (G. Patzelt, pers. comm. 2004). No cold period intense enough to explain the Gschnitz glacier advance was recorded in the pollen above the two younger radiocarbon dates (Patzelt, 1975, 1995).

The Rödschitz peat bog (790 m) lies inside the moraines of the Steinach stadial, but outside Gschnitz stadial moraines of the Traun glacier system (Steiermark, Austria). The basal radiocarbon age of 15 400 ± 470 ^{14}C yr BP (18 020–19 100 cal. yr) (van Husen, 1977, 1997) is a minimum age for the Steinach stadial and indirectly a maximum age for the Gschnitz stadial. The Gschnitz stadial may correspond to a distinct cold phase between 15 400 ^{14}C yr BP and the beginning of the Bølling as identified in the pollen data (Draxler, 1977, 1987). In the same area, two more dates, which were recovered from sediments

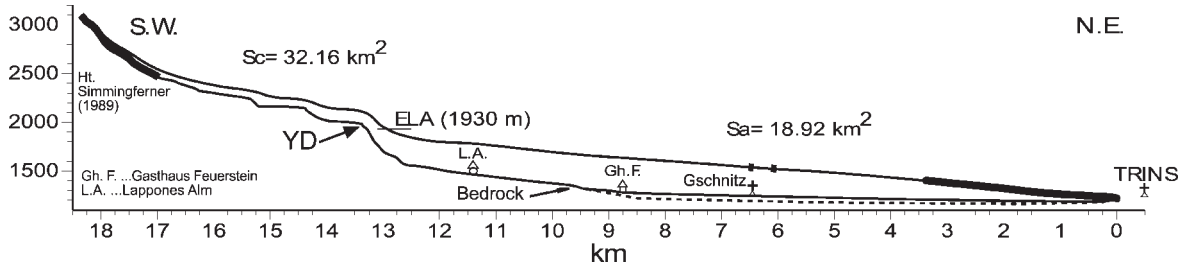

Figure 4 Longitudinal profile of the Gschnitz Stadial glacier. Thick lines at the glacier tongue and above the village of Gschnitz represent preserved moraines. Sc is accumulation area, Sa is ablation area; YD marks position of the Egesen Stadial maximum (Younger Dryas) glacier end (modified from Kerschner *et al.*, 1999)

on the proximal side of Gschnitz moraines, give minimum ages for the local Gschnitz advance of $12\,440 \pm 420$ ^{14}C yr BP (13 950–15 095 cal. yr) and $12\,220 \pm 180$ ^{14}C yr BP (13 835–14 445 cal. yr) (van Husen, 1977; Draxler, 1977, 1987).

To summarise, the published radiocarbon ages indicate that the Gschnitz advance occurred sometime between $15\,400 \pm 470$ ^{14}C yr BP (18 020 $-$ 19 100 cal. yr) (data from Rödschitz peat bog) and $13\,250 \pm 210$ ^{14}C yr BP (15 360–16 015 cal. yr) (data from Lansersee). Pollen data support the pre-Bølling ages. We note the presence of a radiocarbon plateau at about 13 300 ^{14}C yr BP (e.g. Hughen *et al.*, 2004).

Surface exposure dating of the Gschnitz moraine at Trins

Samples for exposure dating were taken from 10 boulders along both lateral moraines as well as at the terminal moraine at Trins (Fig. 3). Seven boulders have been analysed (Table 2). All ^{10}Be data are presented here (Table 3). Quartz veins in the coarse-grained gneiss were sampled with a hammer and chisel. The top centre surface of each boulder was sampled except where indicated below. Quartz vein material was crushed and sieved to <0.8 mm grain size. Quartz mineral separates were purified as well as cleaned of meteoric ^{10}Be following Kohl and Nishiizumi (1992) and Ivy-Ochs (1996). Dissolution of quartz with HF after addition of ^{9}Be, was followed by isolation of Be with ion exchange and selective pH precipitation techniques (Ivy-Ochs, 1996; Ochs and Ivy-Ochs, 1997). ^{10}Be/^{9}Be ratios and appropriate standards and blanks were measured using accelerator mass spectrometry (AMS) following standard procedures at the PSI/ETH Zurich facility (Synal *et al.*, 1997). Subtracted blank ratios were of the order of 1 to 3×10^{-14}.

The surface exposure ages listed in Table 3 were calculated using a sea-level high latitude production rate of 5.1 ± 0.3 ^{10}Be (atoms per gram SiO_2 per year), with 2.6% production due to muon capture (Stone, 2000). Scaling for latitude (geographic) and altitude was based on Stone (2000). No correction has been made for either changes in palaeomagnetic intensity or for non-dipole effects. At this latitude during this time range the effect would have been of the order of 1% or less (Masarik *et al.*, 2001). Topographic shielding was based on a zenith angle dependence of $(\sin\theta)^{2.3}$ (Lal, 1985; Nishiizumi *et al.*, 1989). We have used an exponential depth profile with a rock density of 2.65 g cm^{-3} and an effective attenuation length of 157 g cm^{-2} (cf. Gosse and Phillips, 2001). We estimate the difference between our shielding calculations and those that account for non-perpendicular impingement of cosmic rays on steeply dipping surfaces (cf. Masarik *et al.*, 2000; Dunne *et al.*, 1999) as less than 5%. Note that such corrections would have given smaller effective production rates than the ones we have employed, making the ages slightly older. The errors given for each boulder age reflect analytical uncertainties (dominated by AMS measurement parametres) including $\pm 5^\circ$ on the dip measurement.

We have corrected for snow cover on the flat-topped boulders using 30 cm of snow for 4 months of the year (Fliri, 1975) and a snow density of 0.3 g cm^{-3}. As shown in Table 3, the effect is of the order of 1%. To correct for erosion (weathering) of the rock surface during exposure, we have used an erosion rate of 3.0 ± 0.5 mm kyr^{-1}. This rate is based on the grain-to-grain roughness and overall degree of rounding of the boulders. It is compatible with the erosion rate determined in the Swiss Alpine foreland using ^{10}Be, ^{26}Al and ^{36}Cl measured in a single boulder surface (Ivy-Ochs *et al.*, 2004) and is considered conservative. Bare rock erosion rates of crystalline rocks in alpine environments determined with ^{10}Be and ^{26}Al are generally less than 10 mm kyr^{-1} (e.g. Small *et al.*, 1997).

Table 2 Boulder information: thickness, dip angle of sampled surface and surrounding topography corrections

Boulder no.	Altitude (m)	Boulder diameter (m)	Height above ground (m)	Thickness (cm)	Surface dip angle (degrees)	Dip direction	Shielding correction (topo. only)	Total shielding correction
Gamma 3	1215	2	2	4	44	190	0.985	0.883
Gamma 5	1220	3	1–1.5	4	25	225	0.987	0.888
Gamma 6	1225	2.5	1	2	flat		0.984	0.968
Gamma 7	1220	4	1–2	2	flat		0.986	0.911
Gamma 8a	1215	3	2	2	85	180	0.990	0.538
Gamma 102a	1325	4	2	3	20	10	0.972	0.946
Gamma 103	1330	5	1–2	4	30	120	0.962	0.914

Notes. Total shielding correction includes thickness, dip of rock surface and shielding of surrounding topography, but does not include the snow or erosion corrections.

Table 3 AMS-measured ^{10}Be concentration and calculated exposure ages

Boulder no.	Altitude (m)	^{10}Be atoms/gram	AMS measurement error %	Exposure age (years)	Snow corrected (years)	Exposure age (years) Snow and Erosion corrected (3 mm kyr^{-1})
Gamma 3	1215	1.87×10^5	5.2	14 550 ± 810	14 550	15 110 ± 920
Gamma 5	1220	1.88×10^5	7.2	14 520 ± 1060	14 800	15 380 ± 1130
Gamma 6	1225	1.61×10^5	9.8	11 370 ± 1120	11 570	11 920 ± 1190
Gamma 7	1220	1.76×10^5	8.4	13 220 ± 1120	13 460	13 940 ± 1200
Gamma 8a	1215	1.21×10^5	3.8	15 500 ± 990	15 500	16 130 ± 1040
Gamma 102a	1325	1.94×10^5	4.6	12 940 ± 610	13 180	13 650 ± 650
Gamma 103	1330	2.03×10^5	3.7	14 030 ± 590	14 290	14 830 ± 720

Notes. AMS measurement errors are at the 1σ level, including the statistical (counting) error and the error due to the normalisation to the standards and blanks. Gamma 3 and 8a were not corrected for snow cover as the sampled surfaces were steeply dipping. Final uncertainties in the ages were calculated as described in text.

Boulders 8a, 7 and 3 are located on the left-hand side of the end-moraine complex. Here, there is an abundance of large crystalline boulders separated by kettle holes. Boulder Gamma 8a (16 130 ± 1040 yr) is embedded on the proximal side of the moraine about 10 m below the local moraine crest. We sampled a vertical surface because the top surface was covered with sediment and vegetation. Tree growth on the sampled surface was impossible. In addition, because it is already so low on the moraine ridge, we believe post-depositional exhumation is unlikely. Boulder Gamma 7 (13 940 ± 1200 yr) was sampled along the edge of the top surface. This required an additional shielding correction of 6% (J. Masarik pers. comm., 2004; Masarik and Wieler, 2003). Along one side it is at ground level embedded in the inner side of the moraine, to the proximal side, it is about 2 m above the ground. Unfortunately, we cannot rule out that trees were growing directly on the sampled surface in the past. Boulder Gamma 3 (15 110 ± 920 yr) lies in a topographic low probably related to a kettle hole.

Boulder 5 (15 380 ± 1130) is located on the proximal side of the crest of the terminal moraine. The boulder sticks out from the sediment around 0.5 m on the distal side but more than 1 m on the proximal side. It was also sampled along the edge of the top surface (additional shielding correction of 6%; J. Masarik pers. comm. 2004; Masarik and Wieler, 2003). Boulder Gamma 6 (11 910 ± 1180 yr) was located along the highest part of the terminal moraine, slightly towards the right-hand side. Large in diameter (2.5 m), the boulder appeared very stable, but its top surface was only about 1 m above the enclosing till. The distal slope of the moraine, below the position of the boulder, was undercut by a small stream which comes down from the southern side of the valley (cf. Mayr and Heuberger, 1968). The boulder may have shifted or toppled as a result of this slope undercutting, although this is not apparent today.

Boulders 102a and 103 are found on the right lateral moraine. It is for the most part a single discontinuous ridge that skirts the valley wall 100 m above the valley floor. Boulder 102a (13 650 ± 650) is more than 2 m high and situated right on the crest. The boulder was shattered down the middle but had not broken apart. The pieces appeared to have kept their original orientation, so that we thought we had sampled the original top surface of the boulder. Boulder Gamma 103 (14 230 ± 720) is located a bit farther upstream embedded in the crest of the right lateral moraine.

The calculated exposure ages range from 11 900 to 16 100 years. The simple moraine morphology, volume of sediment, and overall climate history of the Alpine Lateglacial allow us to rule out that the moraine formed over a span of 4200 years. It is also unlikely that the Gschnitz valley glacier was still at the Trins position 11 900 years ago. The Egesen (i.e. Younger Dryas equivalent) moraine of the Gschnitz valley is located some 14 km upvalley (Fig. 4) (Kerschner *et al.*, 1999; Patzelt, pers. comm.) and presumably formed around 12 000 yr ago (Ivy- Ochs *et al.*, 1996, 1999).

The moraine ridge itself is for the most part single-walled and well-defined. It has retained its shape rather well since deposition. Nevertheless, our data indicate that many of the boulders may not have been stable since the glacier abandoned the Trins position or they were covered by sediment during part of their exposure. We note that two of the oldest exposure ages (boulder 3 and boulder 8a) are from the part of the moraine where the glacier was probably covered by crystalline rockfall debris. There, the proportion of very large clasts is much greater, and the proportion of (carbonate) matrix less than on the rest of the moraine. Clast-supported boulders are probably more stable through time as settling and jostling is less. Clearly, we cannot rule out that some of the smaller boulders may have been covered by till part of the time since moraine deposition (cf. Hallet and Putkonen, 1994; Zreda *et al.*, 1994; Putkonen and Swanson, 2003). Finally, the moraine has been forested since the beginning of the Allerød (Bortenschlager, 1984a, 1984b). Trees themselves do not shield cosmic rays significantly (Cerling and Craig, 1994a; Gosse and Phillips, 2001), but they are quite capable of overturning or splitting even very large boulders (cf. Cerling and Craig, 1994b). At Trins, tree roots appear to penetrate the gneiss along the foliation planes, then break off 5–10 cm thick slabs when they fall.

In the light of these factors, our interpretation is that final moraine stabilisation occurred no later than 15 400 ± 1400 yr ago. This is based on the overlapping ages at the older end of the age distribution and is the arithmetic mean of the exposure ages for boulders 3, 5, 8a and 103 (Table 3, Fig. 5). The error reflects the 1σ confidence interval about the mean as well as systematic uncertainties of the production rate (Stone, 2000). We have not included the three younger boulder ages (6, 7 and 102a) as their ages are clearly younger than the independent radiocarbon and pollen constraints for the age of the Gschnitz stadial. These constraints in addition to glacial morphological considerations indicate that Gschnitz stadial glaciers must have downwasted before the Bølling period had even begun (ca. 14 700 yr ago).

Climatic conditions during the Gschnitz stadial

Six kilometres of preserved moraines and other traces of the glacier margin combined with a simple valley topography with

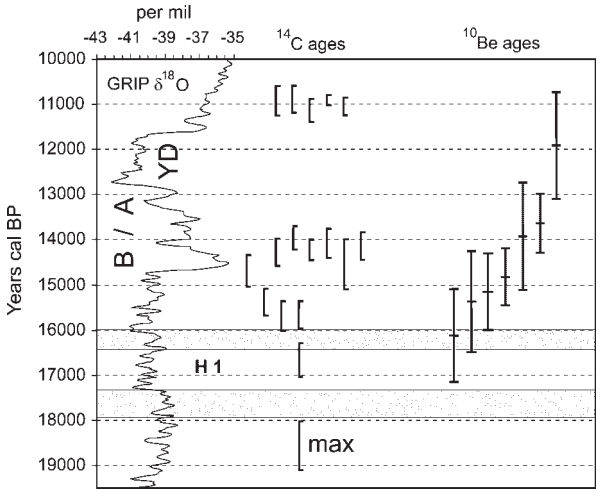

Figure 5 Plot of all ^{10}Be exposure ages for boulders from the Gschnitz stadial moraine at Trins. Based on the four oldest exposure ages, the minimum age for moraine stabilisation is $15\,400 \pm 1100$ yr. This is in accordance with pollen and radiocarbon data from correlative sites in the Alps that indicate a pre-Bølling age for the Gschnitz stadial. Radiocarbon ages were calibrated with IntCal04 (Reimer *et al.*, 2004) using the CALIB 5.0.1 software (Stuiver *et al.*, 1998, 2005). The upper and lower boundaries of Heinrich Event 1 are based on radiocarbon ages from core V23–81 (Bond *et al.*, 1992, 1993; Hemming, 2004). Note that the final calendar ages for the boundaries of H1 are sensitive to ocean reservoir correction applied, which and how the calibration data set is used, and the age–depth model employed, in addition to what lithologic criteria were used to define the H1 layer(s). GRIP oxygen isotope data from Johnsen *et al.* (2001)

an almost perfect parabolic cross-section make the Gschnitz glacier well suited for a palaeoclimatic interpretation with a glacier flow model and a glacier-climate model. The aim is to derive climate sensitive glaciological parametres (ELA, basal shear stress, ablation gradient) and quantitative estimates for precipitation and summer temperature (T_s). The glacier topography is based on both a manual (Kerschner *et al.*, 1999) and a GIS-based reconstruction (Sailer *et al.*, 1999). The glacier flow model and climatic reconstruction calculations presented here are more detailed and straightforward than in an earlier paper (Kerschner *et al.*, 1999).

The ELA, calculated with an accumulation area ratio of 0.57 at 1930 m, was 700 m lower than the LIA ELA in the catchment. The basal shear stress (τ) along the glacier tongue increases from 30 kPa close to the terminus to 70–80 kPa farther upglacier (Kerschner *et al.*, 1999). The small shear stress indicates that the glacier existed in a comparatively dry climatic environment with small mass turnover (Maisch and Haeberli, 1982).

We use the net ablation gradient (change of ablation with altitude: $\partial a/\partial z$) along the glacier tongue as a starting point for the palaeoclimatic interpretation. In a maritime environment it is typically steep (large), indicating a large mass turnover, whereas a flat (small) gradient is typical for a glacier in a cold and dry climate (e.g. Kuhn, 1984; Dyurgerov and Dwyer, 2001). It can be qualitatively compared with those of present-day glaciers and quantitatively interpreted using a glacier-climate model.

The net ablation gradient can be calculated from the reconstructed glacier geometry with a simple glacier flow model (e.g. Murray and Locke, 1989). The model used here is similar to the one used by Oerlemans (1997), Kull (1999) and Kull and Grosjean (2000), assuming steady-state conditions. It calculates ice flux across given cross sections between the ELA and the end-moraine complex. From the difference between the ice flux of two neighbouring cross-sections and the surface area in between, net ablation of the surface increment and $\partial a/\partial z$ can be calculated. The latter is then used to calculate annual precipitation and 'winter precipitation' with statistical relations (see below). These in turn serve as input data for the statistical glacier-climate model by Ohmura *et al.* (1992) and the 'Liestøl equation' (Ballantyne, 1989) to calculate T_s. The assumption of steady state is reasonable, because the overall moraine morphology suggests that the glacier tongue remained stable for decades to centuries.

The necessary equations and variables are given in Table 4. As the driving stress, τ, is small, deformation velocities, sliding velocities and ice fluxes are small as well, resulting in equally small mass balance terms. For calculation of the $a(z)$-curves in Fig. 6, ice flux at a position 8 km upstream from the terminus ('CS8'; glacier surface elevation 1600 m) was calculated first. This is the first cross-section downvalley from the confluence of the main glacier tongue with a tributary glacier from Sandestal and south-facing cirque glaciers. Sliding velocities for the downstream cross-sections were slightly adjusted by a few percent to obtain a reasonably shaped $a(z)$ curve (i.e.

Table 4 Equations for the calculation of ice flow, mass flux and balance gradients (cf. Kull and Grosjean, 2000)

Parameter	Equations and variables
Basal shear stress, τ_b	$\tau_b = \rho g h \sin\alpha \; sf$ ρ, density of ice (900 kg m^{-3}); g, acceleration due to gravity (9.81 m s^{-2}); h, local ice thickness; α, surface slope averaged for $5h$; sf, shape factor for a channel with parabolic cross-section after Nye (1965), optional, depending on scenario
Average ice velocity in cross-section, U	$U = U_d + U_s = f_d \tau^3 \; h + c \; f_s \; \tau^3 / h$ f_d parameter for ice deformation (1.9×10^{-24} Pa^{-3} s^{-1}); f_s parameter for basal sliding (5.7×10^{-20} Pa^{-3} m^2 s^{-1}), f_d and f_s after Budd *et al.* (1979); c correction factor for sliding velocity, depending on scenario
Ice flux through cross-section, Q	$Q = U \; A$ A area of the cross-section
Net ablation between neighbouring cross-sections, a	$a = \Delta Q / S$ S surface area between neighbouring cross-sections

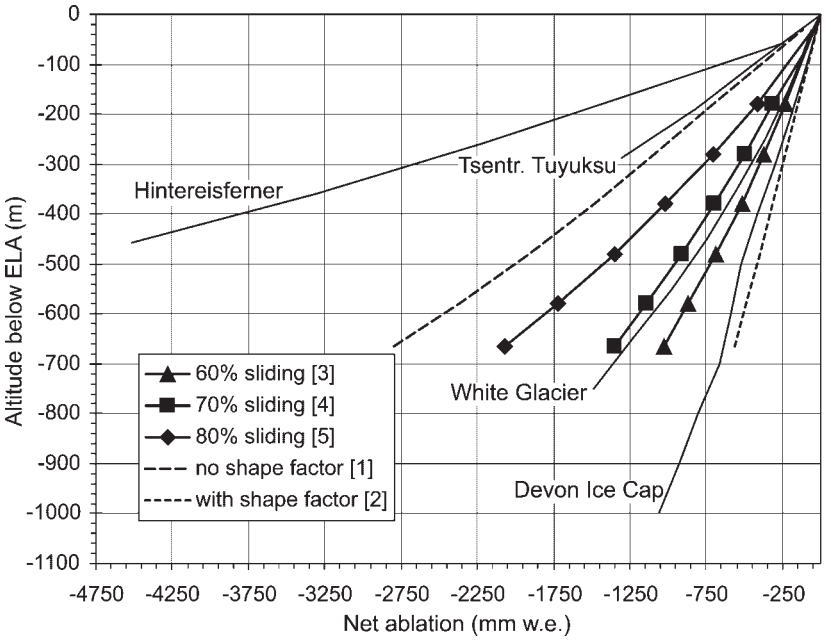

Figure 6 Net ablation gradients of the Gschnitz glacier at the type locality. Numbers in brackets refer to scenarios discussed in the text, w.e stands for water equivalent. Net ablation gradients for modern glaciers from Kuhn (1984)

without kinks). Higher up, the $a(z)$ curve remains fixed at the ELA, where the net balance is zero. Results for various scenarios are discussed below and are summarised in Table 5 and Figure 6.

In the first scenario [1] which is similar to the modelling of Nigardsbreen by Oerlemans (1997), no shape factors were used for the calculation of ice velocities. Owing to the decreasing surface slope towards the end-moraine complex, deformation velocities decrease rapidly downstream. To avoid an inverse $a(z)$ curve, which would indicate a constant decrease of ablation towards the glacier end, sliding velocities downstream from CS8 had to be multiplied by a factor between 2 and 3. This scenario shows the highest mean ice velocities (63 m yr^{-1} at CS8) and hence the highest ablation. However, the valley is narrow and steep-walled with shape factors between 0.55 and 0.7, which cannot be neglected. Therefore, scenario [1] provides an upper boundary for the modelling results. The average ablation gradient is -4.6 kg m^{-2} m^{-1}, which is about half that of present-day Hintereisferner in the Ötztal Alps (Tyrol) and rather similar to that of Tsentraln'yy Tuyuksu Glacier (Tien Shan).

The second scenario [2] provides a lower limit for the modelling results. Both ice deformation and sliding velocities are calculated with shape factors (cf. Kull, 1999; Kull and Grosjean, 2000). Ice velocity is very slow (12.8 m yr^{-1} at CS8) mainly due to very small sliding velocities (30% of the total velocity). Consequently the balance gradient is only -1 kg m^{-2} m^{-1}, which is less than that of Devon Ice Cap in

Table 5 Palaeoglaciologic and paleaoclimatic characteristics of the Gschnitz stadial in central Tyrol, eastern Alps, Austria. 2σ confidence interval for temperatures and temperature depression is ± 1.5 K (for details see text)

Shape factor used: Percent sliding used:	Scenario 1 no 0%	Scenario 2 yes 0%	Scenario 3 yes 60%	Scenario 4 yes 70%	Scenario 5 yes 80%
Mean ice velocity across CS 8, m yr^{-1}	63	13	23	30	45
Ablation gradient, $\partial a/\partial z$ (lowest 300 m of glacier tongue), kg m^{-2} m^{-1}	−4.6	−1.0	−1.8	−2.3	−3.7
Activity index, kg m^{-2} m^{-1}	−4.4	−0.9	−1.8	−2.3	−3.5
Volumetric reaction time (a)	130	620	350	260	170
P at ELA (1930 m), mm yr^{-1}	1140	60	320	480	900
ΔP at ELA (1930 m),%	−21%	−96%	−78%	−67%	−38%
Temperature Jun–Aug/May–Sep					
at ELA (1930 m)	1.4/0.3	−3.3/−8.4	−1.5/−3.4	−0.7/−2.2	0.8/−0.3
at end moraine (1200 m)	6.5/5.4	1.8/−3.3	3.6/1.7	4.4/2.9	5.9/4.8
at Lanser See peat bog (840 m)	9.1/7.9	4.4/−0.8	6.2/4.2	7.0/5.4	8.5/7.3
at Innsbruck (580 m)	10.9/9.8	6.1/1.1	8.0/6.1	8.7/7.3	10.2/9.2
ΔT compared to present ΔT Jun–Aug (Ohmura *et al.*, 1992)	−7.6	−12.3	−10.5	−9.7	−8.2
ΔT May–Sep, 'Liestøl equation'	−7.7	−16.4	−11.5	−10.2	−8.4

the Canadian High Arctic. We consider this scenario unlikely, because the resulting extremely dry and cold climate does not agree with the palaeobotanical record from nearby Lanser See (Bortenschlager, 1984b).

Finally, we calculated three scenarios with shape factors for ice deformation and a contribution of sliding of 60% [3], 70% [4] and 80% [5] of the total velocity. For 60% basal sliding the $a(z)$ curve is between that of Devon Ice Cap and White Glacier (Axel Heiberg Island, Canada), for 70% basal sliding it is similar to that of White Glacier (Cogley *et al.*, 1996). For 80% basal sliding it is already at the upper limit for realistic sliding velocities; the $a(z)$ curve lies between that of Tsentraln'yy Tuyuksu Glacier and White Glacier (Fig. 6).

In all scenarios, the activity index of the glacier (Kuhn and Herrmann, 1990) is practically the same as the balance gradient. Depending on the scenario, the volumetric reaction time (Jóhannesson *et al.*, 1989a,b) of the glacier with a characteristic thickness of 350 m was in the order of 130 to 620 years; for the scenario with 70% sliding it was 260 years. This is much longer than that of similar sized present-day glaciers in the Alps.

For the palaeoclimatological interpretation we use statistical glacier-climate models which relate 'summer temperature' (T_s) at the ELA as the parameter for ablation with 'precipitation' (P) as the parameter for accumulation. We first estimate precipitation from the net balance gradient and then use it as input data to estimate T_s. In this way climatic variables can be entirely derived from the palaeoglaciological record without the need to refer to other proxies.

Ohmura *et al.* (1992) relate precipitation and summer temperature at the ELA of presently existing glaciers on the basis of a worldwide sample. As defined by Ohmura *et al.* (1992), P is the sum of winter accumulation and summer precipitation, and T_s is the free air temperature in summer (June–August) at the altitude of the equilibrium line.

Formally the relation is expressed by the regression equation

$$P = 645 + 296\,T_s + 9\,T_s^2 \quad (1)$$

Reanalysing the data set (Table 3 in Ohmura *et al.*, 1992) with T_s as the dependent variable, the best fit to the data can be obtained with

$$T_s = 0.1815\ P^{0.5} - 4.1\ (R^2 = 0.885) \quad (2)$$

The root mean square error in the relevant part of the equation below 1000 mm of precipitation is 0.8 K. Finally, calculated free air temperatures have to be reduced by 0.6 K to obtain standard climatological temperatures (Kerschner, 2005).

From the ablation gradients of stationary glaciers as used by Kuhn (1984) and the respective precipitation data from Ohmura *et al.* (1992), precipitation at the ELA is

$$P = -14\ (\partial a/\partial z)^2 - 381\ \partial a/\partial z - 321\ (R^2 = 0.978) \quad (3)$$

which is used as input to calculate summer temperature with equation (2). The ablation gradient in equation (3) is taken as the mean of the lowest 300 m of the glacier tongue. For the Gschnitz glacier, calculated values for P (Table 5) range between 1140 mm yr^{-1} (scenario 1) and 60 mm yr^{-1} (scenario 2). The latter value, and therefore also scenario 2, is clearly unrealistic (Fig. 6). For the more realistic scenarios, precipitation at the Gschnitz ELA is between 320 mm yr^{-1} (60% basal sliding) and 900 mm yr^{-1} (80% basal sliding). T_s (equation (2)) at the ELA is between -1.5°C and 0.8°C. Low annual precipitation sums and negative or only slightly positive summer temperatures at the ELA are typical for modern glaciers in the subarctic.

Temperatures for May–September are estimated with the 'Liestøl equation' (Ballantyne, 1989; Nesje and Dahl, 2000; Lie *et al.*, 2003) with 'winter precipitation' (i.e. accumulation) at the ELA as input. As T_s was low, we assume that accumulation at the ELA amounted to at least 90% of precipitation as defined by Ohmura *et al.* (1992).

Then temperature for May to September (Table 5) can be calculated as

$$T_{5-9} = \ln(0.9P/915)/0.339 \quad (4)$$

To calculate temperature and precipitation change, we need to know modern precipitation and temperature at the ELA of the Gschnitz glacier (1930 m). From the data in Fliri (1975), modern (i.e. 1931–1960) T_s at 1930 m (Gschnitz ELA) is 9.0°C. Temperature for May–September is 8°C. Precipitation at the Gschnitz ELA is around 1400 mm yr^{-1}, at the village of Trins (1210 m) close to the end moraine, it is 1000 mm yr^{-1}. Based on these data, annual precipitation at 1930 m during the Gschnitz Stadial was between 20% and 60% of modern values and T_s was between 8 K and 10.5 K lower. Cross-checking with the (P, T) relations by Khodakov (1975) and Krenke (1975), we find similar values for the temperature depression. Temperature depression for May to September was slightly larger than the depression of T_s with values between -8.4°C (80% sliding) and -11.5 °C (60% sliding). In comparison, Younger Dryas precipitation in this area was about 10% less and T_s was 3.5–4 K lower than modern values (Kerschner *et al.*, 2000).

At Lanser See peat bog (840 m), T_s during the Gschnitz stadial was in the order of 6–8.5°C, which is too cold for forest growth. Down in the Inn valley, T_s was probably in the order of 8–10 °C. If we take scenario 4 (70% sliding) as the most realistic scenario, summer climate in the Inn valley 16 000 years ago should have been rather similar to the present-day climatic conditions in drier parts of the subarctic north of the treeline.

Alpine glacier response to cooling associated with H1: the Gschnitz stadial

Moraines from the Gschnitz advance are found predominantly in small to medium-sized catchments (several tens to a few hundred square kilometres). Where the size of the mountains and the morphological situation permits, relict rock glaciers of possible Gschnitz age can be found (Schoeneich, 1998). Notably, moraines of very large glaciers appear to be missing (Rhône valley, the upper Aare valley and its tributaries, or the Swiss/Tyrolean Inn valley), although in the higher areas of the Alps, like the Valais, the Mont Blanc massif or the Bernese Oberland, very large dendritic glacier systems must have still existed. Gschnitz moraines from the large glaciers may be missing in the main valleys for various reasons. One possibility is that the reaction time was just too long for the climatic downturn to result in an advance. On the other hand, the large glaciers may have advanced but the moraines may not have been preserved. This may be the result of bedrock lithologies unfavourable for moraine preservation, subsequent burial of the moraines by valley-fill sediments, or the fact that the glacier termini were calving into the large lakes that existed in the longitudinal valleys during the early Alpine Lateglacial (cf. Poscher, 1993; van Husen, 1997, 2000). In any case, snowline estimates show that, during Gschnitz time, glaciers in these areas must have been very large, consisting of composite dendritic glaciers ending at low altitudes (500–700 m) in the main valleys.

Morphological evidence shows that during the Gschnitz cold period, the glaciers in the Alps advanced over ice-free terrain for several kilometres (van Husen, 1977; Kerschner and Berktold, 1982). This means that a period of pronounced deglaciation preceded the Gschnitz advance. Gschnitz moraines were not built up during a brief stillstand but represent a clear readvance.

To determine when the Gschnitz stadial started, we estimated how long it took the Gschnitz valley glacier to react to the suddenly more severe climatic conditions and then advance to the Trins position. Owing to low mass balance gradients, ablation at the glacier tongue and, thus, the reaction time of the Gschnitz valley glacier was long. A realistic scenario suggests a reaction time of about 300 yr (see also Table 5). The size and the morphology of the Trins moraine suggest that it took at least several decades, perhaps up to a few centuries, to build (Kerschner *et al.*, 2002). In addition, the size and morphology of the lateral moraines indicate a flat palaeoglacier tongue that was likely maintained for decades to centuries. We therefore assume 500 ± 300 years as the amount of time necessary for the glacier to advance, reach and remain at the Trins position. Based on ^{10}Be exposure dates, we know that the Trins moraine finally stabilised at or before $15\,400 \pm 1400$ yr ago. Therefore, the drop in temperature that led to glacier advance and then to formation of the Trins moraine began no later than $15\,900 \pm 1400$ yr ago and probably somewhat earlier.

The time range between 17 000 and 15 000 yr BP, is characterised by abruptly cooler and/or unstable climatic conditions across much of the northern and perhaps the southern hemisphere as well (e.g. Hemming, 2004; Kiefer and Kienast, 2005, and references therein). This is the time period when ice-rafted debris layers that mark Heinrich Event 1 (H1) were deposited (Bond *et al.* 1992, 1993; Broecker and Hemming, 2001; Broecker, 2003; Hemming, 2004) and meridional overturning circulation in the North Atlantic Ocean was greatly reduced (McManus *et al.*, 2004).

Clark and Bartlein (1995) and more recently Licciardi *et al.* (2004) compiled evidence from several sites in North America for a readvance of mountain glaciers ca. 16 000 yr ago, following deglaciation at 21 000–20 000 yr ago. Sites include the Rocky Mountains (Gosse *et al.*, 1995; Licciardi *et al.*, 2001; Benson *et al.*, 2005), the Sierra Nevada (Phillips *et al.*, 1996) and Mount San Gorgonio (Owen *et al.*, 2003) in California. We note that the ^{10}Be ages can be directly compared to ours as they have all been calculated on the same basis (appropriate recalculated ages given in Licciardi *et al.*, 2004). Based on ELA differences, the Gschnitz stadial advance in the Alps represented one-half to two-thirds of that of the LGM glaciers. But Gschnitz stadial glaciers were never the less significantly smaller in volume (Fig. 1). In contrast in western North America, during the 16 000 yr ago readvance mountain glaciers were, in many cases, similar in size to those of the LGM (cf. Owen *et al.*, 2003). Mountain glaciers in the southern hemisphere may have behaved similarly as well (cf. Lowell *et al.*, 1995; Denton *et al.*, 1999; Lowell, 2000; Kaplan *et al.*, 2004).

In northern Europe, ice sheets readvanced markedly several thousand years after abandoning their most extensive LGM positions. For example, the Fennoscandian Ice Sheet (FIS) readvanced to the position marked by the Bremanger moraine between 15 000 and 13 300 ^{14}C yr BP (Nygård *et al.*, 2004). Abandonment of the Bremanger moraine was complete by roughly $13\,320 \pm 340$ ^{14}C yr BP (15 295–16 255 cal. yr). The British Ice Sheet (BIS) readvanced between 14 700 and 13 800 ^{14}C yr BP (around 16 400 cal. yr; McCabe and Clark, 1998; McCabe *et al.*, 1998). These periods of ice sheet expansion overlap the timing we have determined for the Gschnitz stadial.

The suggestion is that early warming evidenced by glacier contraction right after the peak of the LGM (e.g. Lagerklint and Wright, 1999) was interrupted by cooling of the North Atlantic Ocean (e.g. Bard *et al.*, 2000) caused by the fleets of icebergs released during H1 (e.g. Clark *et al*, 2002). Significant cooling of the North Atlantic between approximately 17 000 and 15 000 yr BP (Pietrowski *et al.*, 2004) was recorded as reduced meridional overturning circulation (McManus *et al.*, 2004). Thermohaline circulation in the Norwegian–Greenland Sea was also less vigorous during H1 (Rasmussen *et al.*, 1997; Rasmussen and Thomsen, 2002). Delineation of past permafrost patterns in Europe during intense cold periods, such as the LGM and the Younger Dryas, bears out the association of increased permafrost extent with a cold North Atlantic and abundant pack ice (Renssen and Vandenberghe, 2003) especially in winter (de Vernal *et al.*, 2000). The extremely cold and dry climate that was prevalent during the Gschnitz stadial implies that similar conditions may have existed about 16 000 yr ago. Delivery of warm and moist air masses that at present ameliorate the climate of Europe must have been greatly reduced during H1. The effects of extreme cooling around the time of H1 were felt Europe-wide. Ice sheets in the north expanded (the BIS and the FIS) and valley glaciers in the Alps advanced to form the Gschnitz stadial moraines. Cooling was recorded as well in the Mediterranean region (Cacho *et al.*, 1999, 2001).

Conclusions

Because of the simple shape of the valley and the excellent preservation of the terminal and lateral moraines, the former glacier topography in the Gschnitz valley could easily be reconstructed. Mass balance gradients and statistical glacier-climate models indicate that during the Gschnitz stadial it was cold and dry. The Gschnitz valley glacier was characterised by low mass turnover and negative or only slightly positive summer temperatures at the ELA. This is typical for modern glaciers in the subarctic. For a glaciologically realistic ice flux scenario, precipitation must have been two-thirds less than today and summer temperatures lower by 8.5 to 10 K. This is much colder and drier than it was even during the Younger Dryas. At that time precipitation in this area was only about 10% less and T_s was only 3.5–4 K lower than modern values (Kerschner *et al.*, 2000).

^{10}Be exposure ages for boulders located on the Trins moraine constrain final moraine stabilisation at no later than $15\,400 \pm 1400$ yr ago. Based on palaeoglaciological and glacial-geomorphological constraints we estimate that the glacier advance began about 500 ± 300 yr earlier. This implies that the Gschnitz stadial began no later than $15\,900 \pm 1400$ yr ago. Within the resolution of the dating methods, the Gschnitz stadial is contemporaneous with Heinrich Event 1, a time during which early deglacial warming was slowed or reversed. A very cold North Atlantic Ocean during H1 led to a pause in the delivery of warm moist air masses that today ameliorate the climate of Europe. Thus, the Alps directly record past variations in heat and moisture flux brought by the prevailing westerlies as volume changes in mountain glaciers. Finally, the possibility that H1 was a global phenomenon must not be overlooked, as synchronous glacier advances and/or climatic downturns around 17 000 to 15 000 yr ago have been recorded at numerous sites

worldwide (e.g. Kaplan *et al.*, 2004; Hemming, 2004; Kiefer and Kienast, 2005, and references therein).

Acknowledgements We sincerely thank M. Kaplan and D. van Husen for critical reviews of this manuscript. We would also like to thank G. Patzelt (University of Innsbruck), H. Heuberger (University of Salzburg), M. Maisch (University of Zürich), J. Reitner (Geologische Bundesanstalt, Wien) and L. de Graaff (University of Amsterdam) for insightful discussions. This research was partially funded by Swiss National Fond grant No. 21–043469.95/1 to C. Schlüchter and by Austrian Science Foundation (FWF) grant P-15108 to H. Kerschner. We acknowledge the dedication of the whole accelerator crew. The Zurich AMS facility is jointly operated by the Swiss Federal Institute of Technology, Zurich, and Paul Scherrer Institute, Villigen, Switzerland.

References

Amman B, Lotter AF, Eicher U, Gaillard M-J, Wohlfarth B, Häberli W, Lister G, Maisch M, Niessen F, Schlüchter C. 1994. The Würmian Late-glacial in lowland Switzerland. *Journal of Quaternary Science* **9**: 119–125.

Ballantyne CK. 1989. The Loch Lomond readvance on the Island of Skye, Scotland: glacier reconstruction and palaeoclimatic implications. *Journal of Quaternary Science* **4**: 95–108.

Bard E, Rostek F, Turon J-L, Gendreau S. 2000. Hydrological Impact of Heinrich Events in the Subtropical Northeast Atlantic. *Science* **289**: 1321–1324.

Benson L, Madole R, Landis G, Gosse J. 2005. New data for Late Pleistocene Pinedale alpine glaciation from southwestern Colorado. *Quaternary Science Reviews* **24**: 49–65.

Björck S, Walker MJC, Cwynar C, Johnsen S, Knudsen K-L, Lowe JJ, Wohlfarth B, Intimate Members. 1998. An event stratigraphy for the Last Termination in the North Atlantic region based on the Greenland ice-core record: a proposal by the INTIMATE group. *Journal of Quaternary Science* **13**: 283–292.

Bond G, Heinrich H, Broecker W, Labeyrie L, McManus J, Andrews J, Huon S, Jantschik R, Clasen S, Simet C, Tedesco K, Klas M, Bonani G, Ivy S. 1992. Evidence for massive discharges of icebergs into the North Atlantic Ocean during the last glacial period. *Nature* **360**: 245–249.

Bond G, Broecker W, Johnsen S, McManus J, Labeyrie L, Jouzel J, Bonani G. 1993. Correlations between climate records from North-Atlantic sediments and Greenland ice. *Nature* **365**: 143–147.

Bortenschlager S. 1984a. Beiträge zur Vegetationsgeschichte Tirols I. Inneres Ötztal und unteres Inntal. *Berichte des Naturwissenschaftlich-Medizinischen Vereins in Innsbruck* **71**: 19–56.

Bortenschlager S. 1984b. Die Vegetationsentwicklung im Spätglazial: Das Moor beim Lanser See III. Ein Typprofil für die Ostalpen. *Dissertationes Botanicae* **72**: 71–79.

Broecker W. 2003. Does the trigger for abrupt climate change reside in the ocean or in the atmosphere? *Science* **300**: 1519–1522.

Broecker W, Hemming S. 2001. Climate swings come into focus. *Science* **294**: 2308–2309

Budd WF, Keage PL, Blundy NA. 1979. Empirical studies of ice sliding. *Journal of Glaciology* **23**(89): 157–170.

Burga C. 1980. Pollenanalytische Untersuchungen zur Vegetationsgeschichte des Schams und des San Bernardino-Passgebietes (Graubünden, Schweiz). *Dissertationes Botanicae* **56**: 1–194.

Burga C, Perret R. 1998. *Vegetation und Klima der Schweiz seit dem jüngeren Eiszeitalter*. Ott Verlag: Thun.

Cacho I, Grimalt JO, Pelejero C, Canals M, Sierro FJ, Flores JA, Shackleton N. 1999. Dansgaard-Oeschger and Heinrich event imprints in Alboran Sea paleotemperatures. *Paleoceanography* **14**: 698–705.

Cacho I, Grimalt JO, Canals M, Sbaffi L. 2001. Variability of the western Mediterranean Sea surface temperature during the last 25 000 years and its connection with Northern Hemisphere climate changes. *Paleoceanography* **16**: 40–52.

Cerling TE, Craig H. 1994a. Cosmogenic ^{3}He production rates from 39 °N to 46 °N latitude, western USA and France. *Geochimica et Cosmochimica Acta* **58**: 249–255.

Cerling TE, Craig H. 1994b. Geomorphology and in-situ cosmogenic isotopes. *Annual Review of Earth and Planetary Sciences* **22**: 273–317.

Clark PU, Bartlein PJ. 1995. Correlation of late Pleistocene glaciation in the western United States with North Atlantic Heinrich events. *Geology* **23**: 483–486.

Clark PU, Pisias NG, Stocker TF, Weaver AJ. 2002. The role of the thermohaline circulation in abrupt climate change. *Nature* **415**: 863–869.

Cogley JG, Adams WP, Ecclestone MA, Jung-Rothenhäusler F, Omanney CSL. 1996. Mass balance of White Glacier, Axel Heiberg Island, N.W.T., Canada, 1960–91. *Journal of Glaciology* **42**(142): 548–563.

Denton GH, Heusser CJ, Lowell TV, Moreno PI, Andersen BG, Heusser LE, Schlüchter C, Marchant D. 1999. Interhemispheric linkage of paleoclimate during the last glaciation. *Geografiska Annaler* **81A**: 107–153.

de Vernal A, Hillaire-Marcel C, Turon JL, Matthiessen J. 2000. Reconstruction of sea-surface temperature, salinity, and sea-ice cover in the northern North Atlantic during the last glacial maximum based on dinocyst assemblages. *Canadian Journal of Earth Sciences* **37**(5): 725–750.

Draxler I. 1977. Pollenanalytische Untersuchungen von Mooren zur spät-und postglazialen Vegetationsgeschichte im Einzugsgebiet der Traun. *Jahrbuch der Geologischen Bundesanstalt* **120**: 131–163.

Draxler I. 1987. Zur Vegetationsgeschichte und Stratigraphie des Würmspätglazials des Traungletschergebietes. In *Das Gebiet des Traungletschers, O.Ö. Eine Typregion des Würm-Glazials*, van Husen D (ed.). Mitteilungen der Kommission für Quartärforschung der Österreichischen Akademie der Wissenschaften no. 7; 19–35.

Dunne J, Elmore D, Muzikar P. 1999. Scaling factors for the rates of production of cosmogenic nuclides for geometric shielding and attenuation at depth on sloped surfaces. *Geomorphology* **27**: 3–11.

Dyurgerov M, Dwyer, J. 2001. The steepening of glacier mass balance gradients with northern hemisphere warming. *Zeitschrift für Gletscherkunde und Glazialgeologie* **36**(2000): 107–118.

Fliri F. 1975. *Das Klima der Alpen im Raume von Tirol*. Universitätsverlag Wagner: Innsbruck.

Florineth D, Schlüchter C. 1998. Reconstructing Last Glacial Maximum ice surface geometry and flowlines in the central Swiss Alps. *Eclogae Geologicae Helvetiae* **91**: 391–407.

Florineth D, Schlüchter C. 2000. Alpine evidence for atmospheric circulation patterns in Europe during the Last Glacial Maximum. *Quaternary Research* **54**: 295–308.

Fraedrich R. 1975. Spät-und postglaziale Gletscherschwankungen in der Ferwallgruppe (Tirol/Vorarlberg). *Düsseldorfer Geographische Schriften* **12**: 1–161.

Gosse JC, Klein J, Evenson EB, Lawn B, Middleton R. 1995. Beryllium-10 dating of the duration and retreat of the last Pinedale glacial sequence. *Science* **268**: 1329–1333.

Gosse JC, Phillips FM. 2001. Terrestrial in situ cosmogenic nuclides: theory and application. *Quaternary Science Reviews* **20**: 1475–1560.

Gross G, Kerschner H, Patzelt G. 1977. Methodische Untersuchungen über die Schneegrenze in alpinen Gletschergebieten. *Zeitschrift für Gletscherkunde und Glazialgeologie* **12**(2): 223–251.

Haeberli W. 1991. Zur Glaziologie der letzteiszeitlichen Alpenvergletscherung. In *Klimageschichtliche Probleme der letzten 130 000 Jahre*, Frenzel B (ed.). *Paleoklimaforschung* **1**: 409–419.

Hallet B, Putkonen J. 1994. Surface dating of dynamic landforms: young boulders on aging moraines. *Science* **265**: 937–940.

Hemming S. 2004. Heinrich events: massive late Pleistocene detritus layers of the North Atlantic and their global climate imprint. *Reviews of Geophysics* **42**: 1–43.

Hertl A. 2001. *Untersuchungen zur spätglazialen Gletscher-und Klimageschichte der österreichischen Silvrettagruppe*. PhD dissertation, Universität Innsbruck.

Heuberger H. 1966. *Gletschergeschichtliche Untersuchungen in den Zentralalpen zwischen Sellrain und Ötztal*. Wissenschaftliche Alpenvereinshefte no. 20. Universitätsverlag Wagner: Innsbruck.

Hughen K, Lehman S, Southon J, Overpeck J, Marchal O, Herring C, Turnbull J. 2004. ^{14}C activity and global carbon cycle changes over the past 50 000 years. *Science* **303**: 202–207.

Ivy-Ochs S. 1996. *The dating of rock surfaces using in situ produced ^{10}Be, ^{26}Al and ^{36}Cl, with examples from Antarctica and the Swiss Alps*. PhD dissertation, ETH.

Ivy-Ochs S, Schlüchter C, Kubik PW, Synal H-A, Beer J, Kerschner H. 1996. The exposure age of an Egesen moraine at Julier Pass, Switzerland, measured with the cosmogenic radionuclides ^{10}Be, ^{26}Al and ^{36}Cl. *Eclogae Geologicae Helvetiae* **89**(3): 1049–1063.

Ivy-Ochs S, Schlüchter C, Kubik PW, Denton GH. 1999. Moraine exposure dates imply synchronous Younger Dryas glacier advances in the European Alps and in the Southern Alps of New Zealand. *Geografiska Annaler* **81A**: 313–323.

Ivy-Ochs S, Schäfer J, Kubik PW, Synal H-A, Schlüchter C. 2004. The timing of deglaciation on the northern Alpine foreland (Switzerland). *Eclogae Geologicae Helvetiae* **97**: 47–55.

Jóhannesson T, Raymond C, Waddington E. 1989a. A simple method for determining the response time of glaciers. In *Glacier Fluctuations and Climatic Change*, Oerlemans J (ed.). Kluwer: Dordrecht; 343–352.

Jóhannesson T, Raymond C, Waddington E. 1989b. Time-scale for adjustment of glaciers to changes in mass balance. *Journal of Glaciology* **35**(121): 355–369.

Johnsen SJ, Dahl-Jensen D, Gundestrup N, Steffensen JP, Clausen H, Miller H, Masson-Delmotte V, Sveinbjörnsdottir AE, White J. 2001. Oxygen isotope and palaeotemperature records from six Greenland ice-core stations: Camp Century, Dye-3, GRIP, GISP2, Renland and NorthGRIP. *Journal of Quaternary Science* **16**(4): 299–307.

Kaplan MR, Ackert RP, Singer BS, Douglass DC, Kurz MD. 2004. Cosmogenic nuclide chronology of millennial-scale glacial advances during O-isotope stage 2 in Patagonia. *Geological Society of America Bulletin* **116**: 308–321.

Kelly MA, Buonchristiani J-F, Schlüchter C. 2004. A reconstruction of the Last Glacial Maximum ice-surface geometry in the western Swiss Alps and contiguous Alpine regions in Italy and France: *Eclogae Geologicae Helvetiae* **97**: 57–75.

Kerner von Marilaun F. 1890. Die letzte Vergletscherung der Central-Alpen im Norden des Brenner. *Mittheilungen der kaiserlich-königlichen Geographischen Gesellschaft in Wien* **33**: 307–332.

Kerschner H. 1977. *Das Daun-und Egesenstadium in ausgewählten Tälern der Zentralalpen von Nordtirol und Graubünden*. PhD dissertation, Universität Innsbruck.

Kerschner H. 1986. Zum Sendersstadium im Spätglazial der nördlichen Stubaier Alpen, Tirol. *Zeitschrift für Geomorphologie* **61**(Suppl.): 65–76.

Kerschner H. 1993. Späteiszeitliche Gletscherstände im südlichen Karwendel bei Innsbruck, Tirol. *Innsbrucker Geographische Studien* **20**: 47–55.

Kerschner H. 2005. Glacier-climate models as palaeoclimatic information sources: examples from the Alpine Younger Dryas period. In *Global Change and Mountain Regions (A State of Knowledge Overview)*, Huber UM, Bugmann HKM, Reasoner MA (eds). Springer: Dordrecht; 73–82.

Kerschner H, Berktold E. 1982. Spätglaziale Gletscherstände und Schuttformen im Senderstal, nördliche Stubaier Alpen, Tirol. *Zeitschrift für Gletscherkunde und Glazialgeologie* **17**(2): 125–134.

Kerschner H, Ivy-Ochs S, Schlüchter C. 1999. Paleoclimatic interpretation of the early late-glacial glacier in the Gschnitz valley, Central Alps, Austria. *Annals of Glaciology* **28**: 135–140.

Kerschner H, Kaser G, Sailer R. 2000. Alpine Younger Dryas glaciers as paleo-precipitation gauges. *Annals of Glaciology* **31**: 80–84.

Kerschner H, Ivy-Ochs S, Schlüchter C. 2002. Die Moräne von Trins im Gschnitztal. *Innsbrucker Geographische Studien* **33**(2): 185–194.

Khodakov VG. 1975. Glaciers as water resource indicators of the glacial areas of the USSR. *International Association of Hydrological Sciences Publication* **104**: 22–29.

Kiefer T, Kienast M. 2005. Patterns of deglacial warming in the Pacific Ocean: a review with emphasis on the time interval of Heinrich event 1. *Quaternary Science Reviews* **24**(7–9): 1063–1081.

Kohl CP, Nishiizumi K. 1992. Chemical isolation of quartz for measurement of in-situ produced cosmogenic nuclides. *Geochimica Cosmochimica Acta* **56**: 3583–3587.

Krenke AN. 1975. Climatic conditions of present-day glaciation in Soviet Central Asia. *International Association of Hydrological Sciences Publication* **104**: 30–41.

Kuhn M. 1984. Mass budget imbalances as criterion for a climatic classification of glaciers. *Geografiska Annaler* **66A**(3): 229–238.

Kuhn M, Herrmann A. 1990. Schnee und Eis. In *Lehrbuch der Hydrologie Allgemeine Hydrologie-Quantitative Hydrologie*, Baumgartner A, Liebscher H-J (eds). Borntraeger: Berlin; 271–312.

Kull C. 1999. Modellierung paläoklimatischer Verhältnisse, basierend auf der jungpleistozänen Vergletscherung–ein Beispiel aus den nordchilenischen Anden. *Zeitschrift für Gletscherkunde und Glazialgeologie* **35**(1): 35–64.

Kull C, Grosjean M. 2000. Late Pleistocene climate conditions in the north Chilean Andes drawn from a climate-glacier model. *Journal of Glaciology* **46**(155): 622–632.

Lagerklint IM, Wright JD. 1999. Late glacial warming prior to Heinrich event 1: the influence of ice rafting and large ice sheets on the timing of initial warming. *Geology* **27**: 1099–1102.

Lal D. 1985. Geophysical records of a tree-new applications for studying geomagnetic-field and solar-activity changes during the past 10^4 years. *Meteoritics* **20**(2): 403–414.

Lal D. 1991. Cosmic ray labeling of erosion surfaces: in situ nuclide production rates and erosion models. *Earth and Planetary Science Letters* **104**: 424–439.

Licciardi JM, Clark PU, Brook EJ, Pierce KL, Kurz MD, Elmore D, Sharma P. 2001. Cosmogenic ^{3}He and ^{10}Be chronologies of the late Pinedale northern Yellowstone ice cap, Montana USA. *Geology* **29**: 1095–1098.

Licciardi JM, Clark PU, Brook EJ, Elmore D, Sharma P. 2004. Variable responses of western U.S. glaciers during the last deglaciation. *Geology* **32**: 81–84.

Lie Ø, Dahl SO, Nesje A. 2003. A theoretical approach to glacier equilibrium-line altitudes using meteorological data and glacier mass-balance records from southern Norway. *The Holocene* **13**(3): 365–372.

Lowell TV, Heusser CJ, Andersen BG, Moreno PI, Hauser A, Heusser LE, Schlüchter C, Marchant DR, Denton GH. 1995. Interhemispheric correlation of Late Pleistocene glacial events. *Science* **269**: 1541–1549.

Lowell T. 2000. As climate changes so do glaciers. *Proceedings of the National Academy of Sciences of the United States of America* **97**: 1351–1354.

Maisch M. 1981. Glazialmorphologische und gletschergeschichtliche Untersuchungen im Gebiet zwischen Landwasser-und Albulatal. (Kt. Graubünden, Schweiz.) *Physische Geographie 3*.

Maisch M. 1982. Zur Gletscher-und Klimageschichte des alpinen Spätglazials. *Geographica Helvetica* **37**(2): 93–104.

Maisch M. 1987. Zur Gletschergeschichte des alpinen Spätglazials: Analyse und Interpretation von Schneegrenzdaten. *Geographica Helvetica* **42**(2): 63–71.

Maisch M. 1992. Die Gletscher Graubündens. Rekonstruktion und Auswertung der Gletscher und deren Veränderungen seit dem Hochstand von 1850 im Gebiet der östlichen Schweizer Alpen (Bündnerland und angrenzende Regionen). *Physische Geographie 33*.

Maisch M, Haeberli W. 1982. Interpretation geometrischer Parameter von Spätglazialgletschern im Gebiet Mittelbünden, Schweizer Alpen. In *Beiträge zur Quartärforschung in der Schweiz*, Gamper M (ed.). *Physische Geographie* **1**: 111–126.

Masarik J, Wieler R. 2003. Production of cosmogenic nuclides in boulders. *Earth and Planetary Science Letters* **216**: 201–208.

Masarik J, Kollar D, Vanya S. 2000. Numerical simulation of in situ production of cosmogenic nuclides: effects of irradiation geometry. *Nuclear Instruments and Methods in Physics Research B* **172**: 786–789.

Masarik J, Frank M, Schäfer JM, Wieler R. 2001. Correction of in situ cosmogenic nuclide production rates for geomagnetic field intensity variations during the past 800 000 years. *Geochimica et Cosmochimica Acta* **65**: 2995–3003.

Mayr F, Heuberger H. 1968. Type areas of Lateglacial and Postglacial deposits in Tyrol, Eastern Alps. In *Glaciations of the Alps*, Richmond GM (ed.). *Series in Earth Sciences* no. 7, University of Colorado: Boulder, 143–165.

McCabe MA, Clark PU. 1998. Ice-sheet variability around the North Atlantic Ocean during the last deglaciation. *Nature* **392**: 373–377.
McCabe AM, Knight J, McCarron S. 1998. Heinrich Event I in the British Isles. *Journal of Quaternary Science* **13**: 549–569.
McManus JF, Francois R, Gherardi J-M, Keigwin LD, Brown-Leger S. 2004. Collapse and rapid resumption of Atlantic meridional circulation linked to deglacial climate changes. *Nature* **428**: 834–837.
Müller HN. 1982. Zum alpinen Spätglazial: Das Zwischbergenstadium. *Zeitschrift für Gletscherkunde und Glazialgeologie* **17**(2): 135–142.
Müller HN. 1984. *Spätglaziale Gletscherschwankungen in den westlichen Schweizer Alpen (Simplon-Süd und Val de Nendaz, Wallis) und im nordisländischen Tröllaskagi-Gebirge (Skidadalur)*. Küng: Näfels.
Müller HN, Kerschner H, Küttel M. 1981. Gletscher-und vegetationsgeschichtliche Untersuchungen im Val de Nendaz (Wallis)–ein Beitrag zur alpinen Spätglazialchronologie. *Zeitschrift für Gletscherkunde und Glazialgeologie* **16**(1): 61–84.
Murray DR, Locke WW. 1989. Dynamics of the Late Pleistocene Big Timber Glacier, Crazy Mountains, Montana, U.S.A. *Journal of Glaciology* **35**(120): 183–190.
Nesje A, Dahl SO. 2000. *Glaciers and Environmental Change*. Arnold: London.
Nishiizumi K, Winterer EL, Kohl CP, Klein J, Middleton R, Lal D, Arnold JR. 1989. Cosmic ray production rates of ^{10}Be and ^{26}Al in quartz from glacially polished rocks. *Journal of Geophysical Research* **94**: 17 907–17 915.
Nye JF. 1965. The flow of a glacier in a channel of rectangular, elliptic or parabolic cross-section. *Journal of Glaciology* **5**: 661–690.
Nygård A, Sejrup HP, Haflidason H, Cecchi M, Ottesen D. 2004. Deglaciation history of the southwestern Fennoscandian Ice Sheet between 15 and 13 C-14 ka BP. *Boreas* **33**(1): 1–17.
Ochs M, Ivy-Ochs S. 1997. The chemical behavior of Be, Al, Fe, Ca, and Mg during AMS target preparation modeled with chemical speciation calculations. *Nuclear Instruments and Methods in Physics Research B* **123**: 235–240.
Oerlemans J. 1997. A flowline model for Nigardsbreen, Norway: projection of the future glacier length based on dynamic calibration with the historic record. *Annals of Glaciology* **24**: 382–389.
Ohlendorf C. 1998. *High alpine lake sediments as chronicles for regional glacier and climate history in the Upper Engadine, southeastern Switzerland*. Dissertation, ETH.
Ohmura A, Kasser P, Funk M. 1992. Climate at the equilibrium line of glaciers. *Journal of Glaciology* **38**(130): 397–411.
Owen LA, Finkel RC, Minnich RA, Perez AE. 2003. Extreme southwestern margin of late Quaternary glaciation in North America: timing and controls. *Geology* **31**: 729–732.
Paschinger H. 1952. Die spätglazialen Gletscher des Gschnitztales. *Zeitschrift für Gletscherkunde und Glazialgeologie* **2**(1): 35–57.
Patzelt G. 1972. Die spätglazialen Stadien und postglazialen Schwankungen von Ostalpengletschern. *Berichte der Deutschen Botanischen Gesellschaft* **85**: 47–57.
Patzelt G. 1975. Unterinntal–Zillertal–Pinzgau–Kitzbühel. Spät-und postglaziale Landschaftsentwicklung. In *Tirol–ein geographischer Exkursionsführer*, Fliri F, Leidlmair A (eds). Innsbrucker Geographische Studien: no. 2. Geographisches Institut der Universität: Innsbruck; 309–329.
Patzelt G. 1995. The pollen profile of the peat bog at the Lans lake. 12. Alpine Traverse, Max Maisch. In *Quaternary Field Trips in Central Europe*, Schirmer W (ed.). Pfeil: Munich; 670–671.
Patzelt G, Sarnthein M. 1995. Late Glacial morainal arc at Trins in the Gschnitz valley/Tyrol–'Krotenweiher' peat bog; 12. Alpine Traverse, Max Maisch. In *Quaternary Field Trips in Central Europe*, vol. 2 Schirmer W (ed.). Pfeil: Munich; 669–670.
Penck A, Brückner E. 1901/1909. *Die Alpen im Eiszeitalter*. Tauchnitz: Leipzig.
Phillips FM, Zreda MG, Benson LV, Plummer MA, Elmore D, Sharma P. 1996. Chronology for fluctuations in late Pleistocene Sierra Nevada glaciers and lakes. *Science* **274**: 749–751.
Pichler A. 1859. Beiträge zur Geognosie Tirols. *Zeitschrift des Museums Ferdinandeum Innsbruck* **3**(8): 1–232.
Pietrowski AM, Goldstein SL, Hemming SR, Fairbanks RG. 2004. Intensification and variability of ocean thermohaline circulation through the last deglaciation. *Earth and Planetary Science Letters* **161**: 205–220.
Poscher G. 1993. Neuergebnisse der Quartärforschung in Tirol. In *Geologie des Oberinntaler Raumes–Schwerpunkt Blatt 144 Landeck. Arbeitstagung der Geologischen Bundesanstalt 1993*. Geologische Bundesanstalt: Vienna; 7–27.
Preusser F. 2004. Towards a chronology of the late Pleistocene in the northern Alpine foreland. *Boreas* **33**(3): 195–210.
Putkonen J, Swanson T. 2003. Accuracy of cosmogenic ages for moraines. *Quaternary Research* **59**: 255–261.
Rasmussen TL, Thomsen E. 2002. The role of the North Atlantic Drift in the millenial timescale glacial climate fluctuations. *Palaeogeography, Palaeoclimatology, Palaeoecology* **210**: 101–116.
Rasmussen TL, van Weering TCE, Labeyrie L. 1997. Climatic instability, ice sheets and ocean dynamics at high northern latitudes during the last glacial period (58–10 ka BP). *Quaternary Science Reviews* **16**: 71–80.
Reimer PJ, Baillie MGL, Bard E, Bayliss A, Beck JW, Bertrand CJH, Blackwell PG, Buck CE, Burr GS, Cutler KB, Damon PE, Edwards RL, Fairbanks RG, Friedrich M, Guilderson TP, Hogg AG, Hughen KA, Kromer B, McCormac G, Manning S, Ramsey CB, Reimer RW, Remmele S, Southon JR, Stuiver M, Talamo S, Taylor FW, van der Plicht J, Weyhenmeyer CE. 2004. INTCAL04 Terrestrial radiocarbon age calibration, 0–26 cal kyr BP. *Radiocarbon* **46**: 1029–1058.
Reitner J. 2005. *Quartärgeologie und Landschaftsentwicklung im Raum Kitzbühel-St. Johann i.T.-Hopfgarten (Nordtirol) vom Riss bis in das Würm-Spätglazial (MIS 6-2)*. PhD dissertation, Universität Wien.
Renner F. 1982. *Beiträge zur Gletschergeschichte des Gotthardgebietes und dendro-klimatologische Analysen an fossilen Hölzern*. Physische Geographie *8*, Universität Zürich, Geographisches Institut: Zurich.
Renssen H, Vandenberghe J. 2003. Investigation of the relationship between permafrost distribution in NW Europe and extensive winter sea-ice cover in the North Atlantic Ocean during the cold phases of the Last Glaciation. *Quaternary Science Reviews* **22**(2–4): 209–223.
Sailer R. 2001. *Späteiszeitliche Gletscherstände in der Ferwallgruppe*. PhD dissertation, Universität Innsbruck.
Sailer R, Kerschner H. 1999. Equilibrium line altitudes and rock glaciers in the Ferwall Group (Western Tyrol, Austria) during the Younger Dryas cooling event. *Annals of Glaciology* **28**: 135–140.
Sailer R, Kerschner H, Heller A. 1999. Three-dimensional reconstruction of Younger Dryas glaciers with a raster-based GIS. *Glacial Geology and Geomorphology*, **1999/rp01** (http://ggg.qub.ac.uk/ggg/).
Schlüchter C. 1988. The deglaciation of the Swiss Alps: a paleoclimatic event with chronological problems. *Bulletin. de l'Association Française pour l'étude du Quarternaire* **1988–2/3**: 141–145.
Schlüchter C. 2004. The Swiss glacial record-a schematic summary. In *Quaternary Glaciations—Extent and Chronology, Part I: Europe*, Ehlers J, Gibbard PL (eds). Elsevier: London; 413–418.
Schoeneich P. 1998. *Le retrait glaciaire dans les vallées des Ormonts, de l'Hongrin et de l'Etivaz (Préalpes vaudoises)*. Travaux et recherches *14*, Institut de Géographie, Université de Lausanne: Lausanne.
Senarclens-Grancy WV. 1958. Zur Glazialgeologie des Ötztales und seiner Umgebung. *Mitteilungen der Geologischen Gesellschaft Wien* **49**: 257–313.
Small EE, Anderson RS, Repka JL, Finkel R. 1997. Erosion rates of alpine bedrock summit surfaces deduced from in situ ^{10}Be and ^{26}Al. *Earth and Planetary Science Letters* **150**: 413–425.
Stone JO. 2000. Air pressure and cosmogenic isotope production. *Journal of Geophysical Research—Solid Earth* **105 B10**: 23753–23759.
Stuiver M, Reimer PJ, Bard E, Beck JW, Burr GS, Hughen KA, Kromer B, McCormac G, van der Pflicht J, Spurk M. 1998. INTCAL98 radiocarbon age calibration, 24 000–0 cal BP. *Radiocarbon* **40**: 1041–1083.
Stuiver M, Reimer PJ, Reimer RW. 2005. CALIB 5.0.1 [WWW program and documentation]. 14CHRONO Centre, Queen's University Belfast: Belfast (http://www.calib.org).
Synal H-A, Bonani G, Döbeli M, Ender RM, Gartenmann P, Kubik PW, Schnabel C, Suter M. 1997. Status report of the PSI/ETH AMS

facility. *Nuclear Instruments and Methods in Physics Research B* **123**: 62–68.

Tinner W, Ammann B, Germann P. 1996. Treeline fluctuations recorded for 12 500 years by soil profiles, pollen, and plant macrofossils in the central Swiss Alps. *Arctic and Alpine Research* **28**(2): 131–147.

van Husen D. 1977. Zur Fazies und Stratigraphie der jungpleistozänen Ablagerungen im Trauntal (mit quartärgeologischer Karte). *Jahrbuch der Geologischen Bundesanstalt* **120**: 1–130.

van Husen D. 1997. LGM and Late-glacial fluctuations in the Eastern Alps. *Quaternary International* **38/39**: 109–118.

van Husen D. 2000. Geological processes during the Quaternary. *Mitteilungen der Österreichischen Geologischen Gesellschaft* **92**(1999): 135–156.

van Husen D. 2004. Quaternary glaciations in Austria. In *Quaternary Glaciations—Extent and Chronology*, Part I: Europe, Ehlers J, Gibbard PL (eds). Elsevier: London; 1–13.

Walker MJC, Björck S, Lowe JJ, Cwynar LC, Johnsen S, Knudsen K-L, Wohlfarth B, Intimate Members. 1999. Isotopic 'events' in the GRIP ice core: a stratotype for the Late Pleistocene. *Quaternary Science Reviews* **18**: 1143–1150.

Welten M. 1982. Vegetationsgeschichtliche Untersuchungen in den westlichen Schweizer Alpen: Bern-Wallis. *Denkschriften der Schweizerischen Naturforschenden Gesellschaft* **95**: 1–105.

Wetter W. 1987. Spät-und postglaziale Gletscherschwankungen im Mont-Blanc-Gebiet: untere Vallée de Chamonix-Val Montjoie. *Physische Geographie* **22**: 1–267.

Zoller H, Kleiber H. 1971. Vegetationsgeschichtliche Untersuchungen in der montanen und subalpinen Stufe der Tessintäler. *Verhandlungen der Naturforschenden Gesellschaft Basel* **81**(1): 90–154.

Zreda MG, Phillips FM, Elmore D. 1994. Cosmogenic ^{36}Cl accumulation in unstable landforms 2. Simulations and measurements on eroding moraines. *Water Resources Research* **30**: 3127–3136.